TERT Promoter Mutation Analysis for Blood-Based Diagnosis and Monitoring of Gliomas

Koushik Muralidharan[1], Anudeep Yekula[1], Julia L. Small[1], Zachary S. Rosh[1], Keiko M. Kang[1,2], Lan Wang[1], Spencer Lau[1], Hui Zhang[3], Hakho Lee[4], Chetan Bettegowda[5], Michael R. Chicoine[6], Steven N. Kalkanis[7], Ganesh M. Shankar[1], Brian V. Nahed[1], William T. Curry[1], Pamela S. Jones[1], Daniel P. Cahill[1], Leonora Balaj[1], and Bob S. Carter[1]

ABSTRACT

Purpose: Liquid biopsy offers a minimally invasive tool to diagnose and monitor the heterogeneous molecular landscape of tumors over time and therapy. Detection of *TERT* promoter mutations (*C228T*, *C250T*) in cfDNA has been successful for some systemic cancers but has yet to be demonstrated in gliomas, despite the high prevalence of these mutations in glioma tissue (>60% of all tumors).

Experimental Design: Here, we developed a novel digital droplet PCR (ddPCR) assay that incorporates features to improve sensitivity and allows for the simultaneous detection and longitudinal monitoring of two *TERT* promoter mutations (*C228T* and *C250T*) in cfDNA from the plasma of patients with glioma.

Results: In baseline performance in tumor tissue, the assay had perfect concordance with an independently performed clinical pathology laboratory assessment of *TERT* promoter mutations in the same tumor samples [95% confidence interval (CI), 94%–100%]. Extending to matched plasma samples, we detected *TERT* mutations in both discovery and blinded multi-institution validation cohorts with an overall sensitivity of 62.5% (95% CI, 52%–73%) and a specificity of 90% (95% CI, 80%–96%) compared with the gold-standard tumor tissue–based detection of *TERT* mutations. Upon longitudinal monitoring in 5 patients, we report that peripheral *TERT*-mutant allele frequency reflects the clinical course of the disease, with levels decreasing after surgical intervention and therapy and increasing with tumor progression.

Conclusions: Our results demonstrate the feasibility of detecting circulating cfDNA *TERT* promoter mutations in patients with glioma with clinically relevant sensitivity and specificity.

Introduction

Liquid biopsy for the detection and monitoring of brain tumors is of significant clinical interest. Upon clinical presentation, patients typically undergo imaging followed by biopsy alone or biopsy with resection for diagnosis and determination of histopathologic classification (1). While tissue biopsy is invasive and can, in some cases, be high risk, liquid biopsy can offer a less invasive sampling approach that still affords significant clinical information for diagnosis. In addition, liquid biopsy can be performed more frequently to allow for longitudinal treatment monitoring. The detection of glioma mutations via liquid biopsy of cerebrospinal fluid has been demonstrated (2–6); however, the ability to detect mutations in cell free DNA (cfDNA) in plasma with similar sensitivities has been limited to date (5, 7, 8).

TERT promoter mutations are among the most common genetic alterations in glioma (6, 9, 10).The two most common mutations are *C228T* (45% of all *TERT* promoter mutations) and the *C250T* (15% of all *TERT* promoter mutations), occurring 124 and 146 bp, respectively, upstream of the *TERT* transcriptional start site (11). These mutations are typically heterozygous, mutually exclusive, and due to the GC-rich nature of the promoter, yield an identical 11bp "CCCGGAAGGGG" ETS/TCF binding motif that is associated with increased transcriptional activity of *TERT*, and therefore increased telomerase activity (12, 13). Somatic mutations in *TERT* promoter are common across all grades of gliomas with a frequency of 8% in pilocytic astrocytomas (grade I), 15% in diffuse astrocytomas (grade II), 45% in oligodendrogliomas (grade II), 54% in anaplastic oligodendrogliomas (grade III), and 62% in glioblastoma (grade IV; refs. 9, 10, 14, 15). Notably, the presence of *TERT* promoter mutation is a poor prognostic marker in high-grade *IDH* wild-type glioblastoma (9, 10, 15), but *TERT* promoter mutation confers a positive prognosis in lower grade tumors, distinguishing between *TERT*/*IDH* comutated oligodendroglioma and *IDH*-mutant astrocytoma (9). To date, PCR amplification of *TERT* has proven technically difficult due to the high GC content in the promoter region (>80%; refs. 16, 17). To address these issues, several additive and nonadditive-based approaches including Q-sol, 7-deaza-dGTP, and locked nucleic acid (LNA)-enhanced probes have been reported previously (11, 18–20).

In this report, we describe the development of a novel ddPCR probe-based assay (**Fig. 1A**) that can detect two *TERT* promoter mutations (*C228T* and *C250T*) in the plasma of glioma patients simultaneously.

[1]Department of Neurosurgery, Massachusetts General Hospital and Harvard Medical School, Boston, Massachusetts. [2]School of Medicine, University of California, San Diego, La Jolla, California. [3]Biostatistics, Massachusetts General Hospital and Harvard Medical School, Boston, Massachusetts. [4]Center for Systems Biology, Massachusetts General Hospital and Harvard Medical School, Boston, Massachusetts. [5]Department of Neurosurgery, Johns Hopkins Medical Institutions, Baltimore, Maryland. [6]Department of Neurosurgery, Washington University Medicine in St. Louis, St. Louis, Missouri. [7]Department of Neurosurgery, Henry Ford Health System, Detroit, Michigan.

Note: Supplementary data for this article are available at Clinical Cancer Research Online (http://clincancerres.aacrjournals.org/).

L. Balaj and B.S. Carter are the co-senior authors of this article.

Corresponding Authors: Leonora Balaj, Massachusetts General Hospital, 185 Cambridge Street, Boston, MA. E-mail: Balaj.Leonora@mgh.harvard.edu. Phone: 617-726-3454; and Bob S. Carter, E-mail: Bcarter@mgh.harvard.edu

Clin Cancer Res 2021;27:169–78

doi: 10.1158/1078-0432.CCR-20-3083

Translational Relevance

TERT promoter mutations are highly prevalent in gliomas (>60%), with the highest incidence in primary glioblastomas (>80%). Detection and quantification of *TERT* promoter mutations in cell-free DNA (cfDNA) have been previously investigated for several systemic cancers with limited success but have not been applied to CNS tumors. Here, we developed a digital droplet PCR assay for the detection of *TERT* promoter mutations in cfDNA from the plasma of patients with gliomas, independently in discovery and blinded multi-institution validation ($n = 157$) cohorts, with a sensitivity of 62.5% and specificity of 90%. In addition, we show that all patients within our study cohort with an abnormal MRI and a *TERT*-mutant allele frequency above threshold were diagnosed with glioma. We also show that levels of peripheral *TERT*-mutant allele frequency rise and fall corresponding to clinical course in a small longitudinal cohort ($n = 5$).

In an analysis of totaling 157 patients, we describe the sensitivity of this assay for detecting *TERT* promoter mutations in plasma, and highlight potential clinical applications, for diagnosis and therapeutic monitoring of glial tumors using this blood test.

Materials and Methods

Study population

The study population ($n = 157$) included patients 18 years or older with pathology confirmed *TERT* mutant or wild-type gliomas who underwent surgery at either the Massachusetts General Hospital (MGH, Boston, MA), Henry Ford Health System (HFHS), or at Washington University St. Louis (WUStL, ST. Louis, MO) and age-matched healthy controls (**Fig. 2A**; **Table 1**).The study population was divided into a discovery cohort ($n = 83$; 46 *TERT* mutant, 17 *TERT* wild-type, 20 matched healthy controls) and a blinded multi-institution validation cohort ($n = 74$; 42 *TERT* mutant, 9 *TERT* WT, 14 matched healthy controls, 9 nontumor MRI positive). For glioma cohorts, exclusion criteria consisted of history of other primary or metastatic cancers, active infectious disease, current or previous enrollment in clinical trials, and hemolyzed plasma samples. All healthy control subjects were screened for pertinent oncologic and neurologic medical histories. Individuals with a history of cancer, neurological disorders, and infectious diseases were excluded from the study. All samples were collected with written informed consent after the patient was advised of the potential risks and benefits, as well as the investigational nature of the study. Our studies were conducted in accordance with principles for human experimentation as defined in the U.S. Common Rule and were approved by the Human Investigational Review Board of each study center under Partners institutional review board (IRB)-approved protocol number 2017P001581. BRISQ guideline reports are included in Supplementary Table S1. Samples were taken from patient population undergoing treatment at MGH, HFHS, or WUStL. Some samples may still be available and could be shared with appropriate documentation (IRB, MTA etc.). ExoLution PLUS is a proprietary kit available from Exosome Diagnostics (a BioTechne brand).

Tumor tissue processing

Tumor tissue was microdissected and suspended in RNAlater (Ambion) or flash-frozen and stored at −80°C.

Patient plasma processing

Whole blood was collected using K2 EDTA tubes with an inert gel barrier (BD Vacutainer Blood Collection Tubes), from preoperatively placed arterial lines or venipuncture. Within 2 hours of collection, samples were centrifuged at 1,100 × *g* for 10 minutes at 20°C to separate the plasma from the hematocrit and filtered using 0.8-μm filters. One-milliliter aliquots were stored at -80°C for later downstream analysis. With the exception of the longitudinal samples, all baseline samples were collected prior to surgical resection.

Cell lines

Human carcinoma cell line A431 (ATCC CRL-1555; RRID: CVCL_0037) was cultured in DMEM with high glucose (DMEM; Gibco, Invitrogen Cell Culture), containing 10% FBS (Life Technologies Corporation) and 1% penicillin/streptomycin (Life Technologies). Human glioma cell line U87 (ATCC HTB-14; RRID: CVCL_0022) was cultured in DMEM with high glucose, containing 10% FBS and 1% penicillin/streptomycin. Human brain microvascular endothelial cells (HBMVEC) were kindly provided by Xandra O. Breakefield (Massachusetts General Hospital, Boston, Massachusetts) and cultured using endothelial basal medium (EGM-2 MV Microvascular Endothelial Cell Growth Medium-2 BulletKit, Lonza). All cell lines were grown to 50%–70% confluency prior to gDNA extraction to minimize cell death and optimize quality of gDNA. All cell lines were verified monthly using the Mycoplasma PCR detection kit (Applied Biological Materials) to ensure lack of *Mycoplasma* contamination. All cell lines were obtained from ATCC, and were used within ten passages within the time of thawing.

DNA isolation

DNA was isolated from cell lines and frozen tumor tissue using the DNeasy Blood and Tissue Kit (Qiagen) as recommended by the manufacturer. DNA was eluted in AE buffer (Qiagen) and stored at −20°C until further processing. DNA concentration and purity were determined using the NanoDrop One (ThermoFisher Scientific).

Plasma cfDNA isolation

Circulating nucleic acid was extracted from plasma using the QIAamp Circulating Nucleic Acid Kit (Qiagen) or ExoLution PLUS (Exosome Diagnostics) as per the manufacturer's instructions. cfDNA eluted in 20 μL AVE buffer (QIAamp Circulating Nucleic Acid Kit) or in 20 μL nuclease-free water (ExoLution PLUS Kit) and stored at −20°C until quantification and subsequent ddPCR test.

TERT ddPCR assay

Because both the *C228T* and *C250T TERT* promoter mutations yield the same sequence (**Fig. 1B**), a single probe was used to detect both mutations. A second probe was also used to recognize the C228 wild-type locus. As described by McEvoy et. al, Locked Nucleic Acid (LNA) modifications were introduced on probes due to the short size of the probe, indicated by "+" (20). The sequences for the probes used are as follows: *TERT* promoter mutant (5′-FAM/CCC +C+T+T+CCGG/3IABkFQ/) and *TERT* promoter wild-type (5′-HEX/CCC C+C+T +CCG G/3IABkFQ/). Probes were synthesized by Integrated DNA Technologies (IDT). ddPCR amplification was performed using either 4 μL of cfDNA template or using 100 ng of tumor gDNA, 1× ddPCR Supermix for probes (no dUTP, Bio-Rad), either 1× Q-sol or 200 mmol/L 7-deaza-dGTP (7dG; New England Biolabs), 250 nmol/L of each probe, and 900 nmol/L of each primer (5′-CCTGCCCCTTCACCTTCCAG-3′ and 5′-AGAGCGGAAAG-GAAGGGGA-3′) with template (100 ng of tumor tissue or 4 uL of

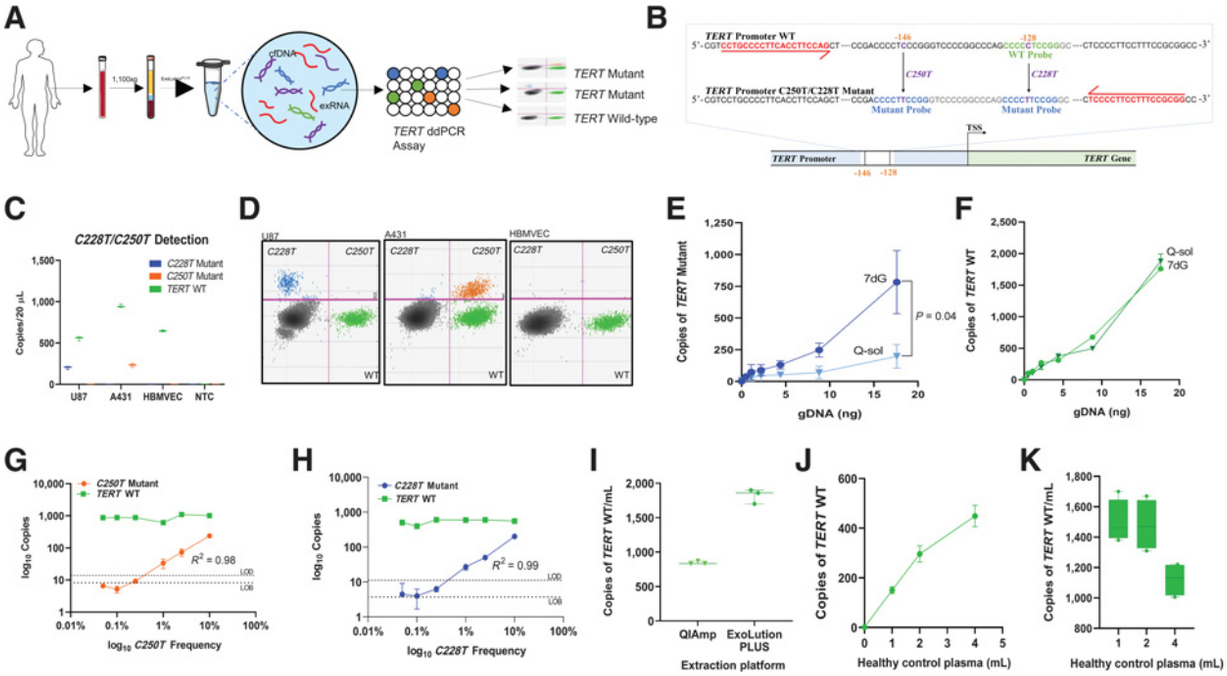

Figure 1.

Overview and optimization of *TERT* promoter mutation ddPCR assay. **A,** Schematic depicting experimental workflow, including isolation of plasma, extraction platform, and *TERT* promoter ddPCR readout. **B,** *TERT* promoter nucleotide sequence illustrating forward and reverse primers as well as probes specific to each mutation. **C,** Absolute quantification of *TERT* mutant copies from equal inputs of genomic DNA from U87 (*C228T*), A431 (*C250T*), and HBMVEC (WT) cell lines. **D,** 2D amplitude plots indicate the mutant and wild-type populations for each specific mutation and cell line. The *y*-axis indicates positivity in the mutant channel, and the *x*-axis indicates positivity in the wild-type channel. Events positive for both channels are shown in the upper right corner of the 2D amplitude plot. Both mutant and wild-type probes can bind the *C250T* mutation, due to the location of the point mutation (positive in the bottom and top right corner). However, either the wild-type probe or the mutant probe can exclusively bind to the *C228T* mutation (positive in the top left and bottom right corner). Background signal is seen in the bottom left corner. Serial dilutions of genomic DNA (gDNA) from A431 cells are used as templates for *TERT* ddPCR assay using 7-deaza-dGTP Q-sol as an additive. Copies per 20 µL of *TERT* mutant (**E**) and *TERT* WT (**F**) are plotted against input (in nanograms) of A431 gDNA. Serial dilutions of gDNA from *TERT* mutant cell lines U87 (*C228T*; **G**) and A431 (*C250T*; **H**) were diluted in a constant background of *TERT* WT HBMVEC gDNA from 10% mutant allele frequency to 0% mutant allele frequency. Copies per 20 µL of *TERT* Mutant and *TERT* WT are plotted against mutant allele frequency. Limit of detection (LOD, dashed line) is plotted, defined as 2 standard deviations over the mean frequency abundance obtained at 0% when only *TERT* WT DNA was used as input. Limit of blank (LOB, dotted line) is plotted, defined as the highest apparent mean frequency abundance expected to be found when replicates of a blank sample containing no *TERT* Mutant copies are tested. **I,** cfDNA was extracted from 2 mL of healthy control plasma using the QIAmp circulating nucleic acid kit (Qiagen) and the ExoLution PLUS extraction kit (Exosome Diagnostics). Two microliters of cfDNA was used as input for absolute quantification of *TERT* WT cfDNA. Copies/mL were calculated using the formula described in Methods. cfDNA was extracted from 1, 2, and 4 mL of healthy control plasma using the ExoLution PLUS kit (Exosome Diagnostics). Two microliters of cfDNA was used as input for absolute quantification of *TERT* WT cfDNA. Copies per 20 µL (**J**) and copies/mL (**K**) are plotted against the amount of healthy control plasma used for reaction.

cfDNA) in a total reaction mix of 20 µL. The QX200 manual droplet generator (Bio-Rad) was used to generate droplets. Thermocycling conditions were as follows: 95°C (51% ramp) for 10 minutes, 40 cycles of 94°C (51% ramp) for 30 seconds, and 57°C for 1 minute, followed by 98°C for 10 minutes and held at 4°C until further processing. Droplets were counted and analyzed using the QX200 droplet reader (Bio-Rad) and QuantaSoft analysis (Bio-Rad) was performed to acquire data.

Quantification of copies/mL of plasma

Copies per mL of plasma is calculated by taking copies/20µL (C; provided by QuantaSoft), multiplied by elution volume in µL (EV), divided by the total volume added to the reaction (TV), divided by the plasma volume (PV). In short, Copies/mL of plasma = C*EV/TV/PV.

R-based ddPCR analysis of MAF from plasma samples

Gates were constructed for both channel 1 (4–8) and channel 2 (2–6) in increments of 0.05. Combinations of channel 1 gates and channel 2 gates were used to calculate MAF, the number of channel 1–positive droplets divided by the number of channel 2 positive droplets. Thresholds were calculated to fulfill one of the following criteria: maximize specificity, set specificity close to 90%, and to minimize the distance from the ROC curve to the point (0,1). These gating strategies (trained using a discovery cohort) were then used to analyze the data from the multi-institution validation cohort in a blinded fashion. Code available on GitHub Repository koushikmuralidharan/BILL.

Statistical analysis

Statistical analyses were performed using unpaired two-tailed Student *t* test in GraphPad Prism 8 software and $P < 0.05$ was considered statistically significant. Confidence intervals were calculated using exact binomial distributions. The results are presented as the mean ± SD. "***" indicates *P* value less than or equal to 0.001, and "****" indicates *P* value less than or equal to 0.0001.

Data/code availability statement

Source data for figures are provided within supplementary figures. Code is available on GitHub Repository koushikmuralidharan/BILL.

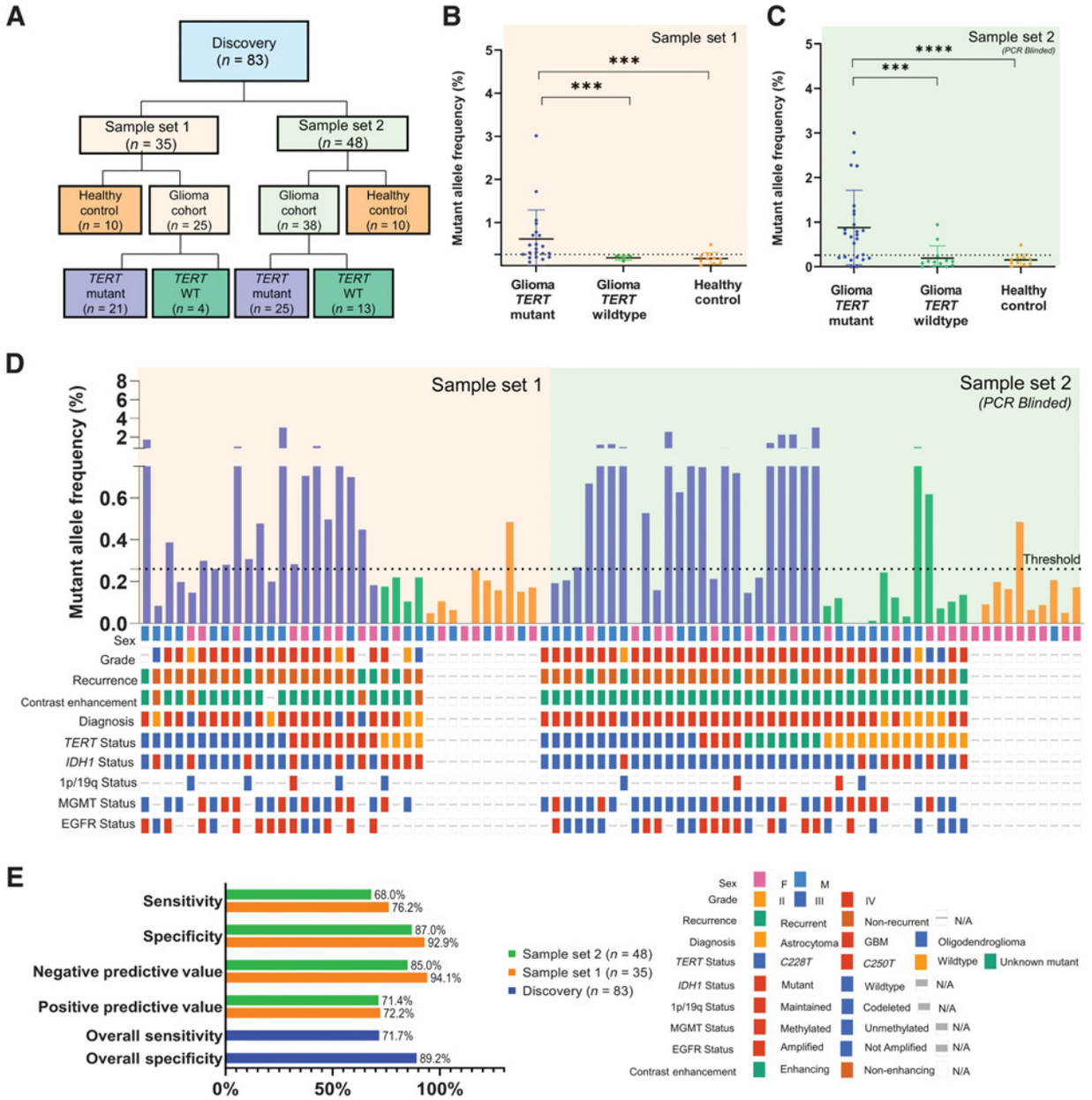

Figure 2.

Detection of *TERT* promoter mutation in plasma of Discovery Cohort. **A,** CONSORT diagram depicting patient cohorts and overall study design. **B,** cfDNA from 2 mL of matched patient plasma from patient cohort 1 (21 *TERT* Mutant and 4 *TERT* WT; $n = 25$) and healthy control (*TERT* WT; $n = 10$) was used as input for absolute quantification of *TERT* mutant (*C228T* or *C250T*) and wildtype copies. **C,** Plasma samples from PCR blinded sample set 2 (25 *TERT* Mutant and 13 *TERT* WT; $n = 38$) and healthy control (*TERT* WT; $n = 10$) were used as input for absolute quantification of *TERT* mutant (*C228T* or *C250T*) and analyzed using parameters established in sample set 1. All data are shown in MAF, calculated using the formula described in Methods and Supplementary Fig. S2. MAF of *TERT* Mutant for plasma samples are plotted against cohort sub-classification. Dotted line indicates a threshold of 0.26% MAF, used to designate samples as *TERT* Mutant positive or negative. **D,** MAF of *TERT* Mutant is graphed according to sample number. Oncoprint depicting the genomic landscape of each sample is plotted underneath. **E,** Contingency tables were constructed from data obtained, and sensitivity and specificity were calculated and graphed above. Overall sensitivity and specificity across both sample sets ($n = 83$) are also reported. ***, $P < 0.001$.

Results

Assay design and optimization

The most common *TERT* promoter mutations, *C228T* and *C250T*, are heterozygous and mutually exclusive, but both mutations result in the generation of an 11-bp identical sequence, 5′-CCCCTTCCGGG-3′. We used a 10-bp LNA-mutant probe to simultaneously detect both mutations and an LNA wild-type probe complementary to the C228 locus (**Fig. 1B**). Assay specificity for each mutation was established using U87 (*C228T* mutant), A431

Table 1. Patient demographics.

	Discovery Set 1	%	Discovery Set 2	%	Blinded Multi-institution Validation Cohort	%
Total	35		48		74	
Disease Group Age median, IQR	50 (43–64)		59.5 (50–68.5)		56 (46–66.5)	
Healthy Group Age median, IQR	31.5 (26–52.75)		26.5 (24–29.75)		55.5 (48.5–63.3)	
Non-Tumor Group Age median, IQR	N/A		N/A		66 (62–67)	
Sex						
Male	16	45.7	25	52.1	46	62.2
Female	19	54.3	23	47.9	28	37.8
Race, *n* (%)						
White	31	88.6	43	89.6	65	87.8
Asian	1	2.9	2	4.2	3	4.1
Black	0	0.0	0	0.0	3	4.1
Other	2	5.7	1	2.1	0	0.0
Unavailable	1	2.9	2	4.2	3	4.1
Ethnicity, *n* (%)						
Hispanic	1	2.9	2	4.2	0	0.0
Non-Hispanic	30	85.7	40	83.3	55	74.3
Unavailable	4	11.4	6	12.5	19	25.7
WHO Grade, *n* (%)						
II	3	8.6	2	4.2	2	2.7
III	3	8.6	4	8.3	10	13.5
IV	16	45.7	32	66.7	33	44.6
N/A	13	37.1	10	20.8	29	39.2
Disease status						
Newly diagnosed	21	60.0	30	62.5	39	52.7
Recurrent	4	11.4	8	16.7	18	24.3
N/A					17	23.0
Medications, *n* (%)						
Anticonvulsants (levetriacetam, clonazepam, lacosamide, carbamazepine, lamotrigine)	16	45.7	13	27.1	30	40.5
Steroids (dexamethasone)	7	20.0	10	20.8	18	24.3
Blood thinner (aspirin, coumadin)	3	8.6	4	8.3	9	12.2
Prior radiotherapy	1	2.9	5	10.4	2	2.7
Prior chemotherapy	2	5.7	8	16.7	4	5.4
Clinical trial participant	1	2.9	1	2.1	6	8.1

Abbreviations: IQR, interquartile range; N/A, not applicable.

(*C250T* mutant), and HBMVEC (*TERT* WT) gDNA (**Fig. 1C**). For inputs with mutant allele frequencies (MAF) greater than 10%, 2D amplitude analysis can distinguish between *C250T*/*C228T* mutations (**Fig. 1D**; Supplementary Fig. 1A). *TERT* promoter mutations are situated in a GC-rich region resistant to amplification that hinders assay performance. To stabilize amplification, we compared Q-sol additive to 7-deaza-dGTP (7dG), a modified nucleotide that inhibits secondary structure formation (17). *TERT* assay performance with 7dG was superior to Q-Sol (1.8–3.9-fold increase, $P = 0.04$) with higher absolute mutant detection and comparable WT detection (**Fig. 1E** and **F**). We report analytical parameters including limit-of-detections (LODs) of 0.27% MAF (*C250T*) and 0.42% (*C228T*) MAF and limit of blanks of 0.02% (*C250T*) and 0.04% MAF (*C228T*; **Fig. 1G** and **H**; Supplementary Fig. S1). In a comparison of extraction platforms to optimize *TERT* recovery, a 2-fold increase in *TERT* WT ($P = 0.001$) was seen while using ExoLution PLUS in comparison with the QiAmp Circulating Nucleic Acid kit (Qiagen; **Fig. 1I**). Two milliliters of plasma was determined to be the optimal input for recovery as a function of copies of *TERT* WT per mL of plasma (**Fig. 1J** and **K**).

Development of R-based analysis for *TERT* promoter ddPCR analysis and cohort design

To standardize gating without operator bias, we sought to mathematically define and automate the gating strategy. Our gating strategy is based on the algorithm used by the R-program ddPCR, which defines empty droplets as those that lie within 7 SDs above the mean amplitude of channel 1 (21). To determine the optimal gating strategy, we gated continuously from 4–8 SDs above the mean amplitude of channel 1 and 2–6 SDs above the mean amplitude of channel 2 in increments of 0.05, with pseudocode provided in Supplementary Fig. S2. Bootstrapping with 1000 replicates was used to determine a threshold, and a list of gating strategies with threshold values was generated to ensure that specificity was greater than or equal to 90%. We present one such gating strategy that maximizes the sum of discovery sensitivity, validation sensitivity, and overall sensitivity. This gating strategy gates at 7.15 SDs above the mean of channel 1 amplitude, 2.95 SDs above the mean of channel 2 amplitude, with a threshold of 0.26% MAF (Supplementary Fig. S2). This is in accordance with prior literature, which suggests that positive droplets lie 7 SDs above the mean amplitude of channel 1 (21). Notably, the threshold calculated by the program, 0.26% MAF, was equivalent to the experimentally

determined LOD (MAF) of the *TERT* Promoter ddPCR Assay using cell line derived gDNA (**Fig. 1G**).

Detection of *TERT* promoter mutations in cfDNA from discovery and blinded validation cohort

We selected a cohort ($n = 157$) of molecularly characterized glioma patients ($n = 114$), nontumor patients with enhancing lesions on MRI ($n = 9$), and age matched healthy controls ($n = 33$). Our patient population spanned tumor diagnosis (20% astrocytoma, 7% oligodendroglioma, 72% glioblastoma, 1% gliosarcoma); grade (6% II; 15% III, 71% IV, 8% not reported) and molecular characteristics: *IDH1* mutant (19%), *TERT* mutant (45% *C228T*; 15% *C250T*), 1p19q codeletion (7%), EGFR amplified (20%), MGMT methylated (33%; **Table 1**; **Fig. 2**). The study population was randomly assigned to either a discovery cohort ($n = 83$) or a blinded multi-institutional validation cohort ($n = 74$). To assess the clinical performance of the assay, tumor tissue and matched plasma samples were analyzed for the presence of the *TERT* mutations (Supplementary Fig. S3).

In tissue, we demonstrated that our assay and the CLIA certified Solid SNAPSHOT assay (22) used in the MGH Department of Pathology, detected *TERT*-positive tumors with 100% concordance across 97 tested samples for the presence of the *TERT* promoter mutation. (**Fig. 2A**; Supplementary Fig. S3). In one patient, using parallel tumor tissue aliquots, our assay detected the *C250T* mutation while the SNAPSHOT assay detected the *C228T* mutation.

Plasma samples (total $n = 83$; *TERT* mutant $n = 46$; *TERT* WT $n = 17$; healthy controls $n = 20$) were analyzed and gated (Supplementary Fig. S2) in two separate discovery sample sets (**Fig. 2A**). In sample set 1, we report positivity in 16 of 21 (76%) *TERT*-mutant samples, and in 1 of 14 (7%) WT control samples (**Fig. 2B**), with a sensitivity of 76.19% (CI, 52.83–91.78), and specificity of 92.86% (CI, 66.3–99.82). In sample set 2 (PCR blinded), we report positivity in 17 of 25 (68%) of *TERT*-mutant samples, and in 3 of 20 (15%) of WT control samples (**Fig. 2C**), with a sensitivity of 68.00% (CI, 46.50–85.05), and specificity of 86.96% (CI, 66.41–97.22). Overall, in the discovery cohort, we report positivity in 33 of 46 (72%) *TERT*-mutant samples, and in 4 of 37 (11%) *TERT* WT samples (**Fig. 2D**), with a sensitivity of 71.74% (CI, 56.54–84.01) and specificity of 89.19% (CI, 74.58–96.97).

To validate assay performance in multi-institutional samples, we analyzed a blinded cohort [total $n = 74$; *TERT* mutant $n = 41$ (Henry Ford Hospital $n = 12$; Washington University $n = 2$; Massachusetts General Hospital $n = 27$); *TERT* WT $n = 17$; healthy control $n = 14$, CNS disease nonglioma $n = 9$] using the parameters previously described (**Fig. 3A**; Supplementary Fig. S2). The CNS disease nontumor samples are from patients who either had a nonmalignant contrast enhancing mass on MRI, such as a demyelinating lesion or fungal abscess, that was initially suspected as glioma or other nontumor conditions such as normal pressure hydrocephalus. In matched plasma, we report positivity in 22 of 42 (52%) confirmed mutant samples and 3 of 33 (9%) confirmed wild-type with a sensitivity of 52.38% (CI, 36.42%–68.00%), specificity of 90.91% (CI, 75.67%–98.08%; **Fig. 3B–D**).

The blinded multi-institution validation cohort verifies and validates our assay performance for the detection of the *TERT* promoter mutation in plasma (23–25). In summary, combining all three cohorts ($n = 157$), we demonstrate a sensitivity of 62.50% (CI, 51.53%–72.60%), and a specificity of 90% (CI, 80.48%–95.8%; **Figs. 2E** and **3D**). Of patients who were classified positive by plasma analysis but negative by tissue analysis at the MAF threshold selected, the clinical scenario of these false positive samples included 4 of 34 healthy controls, 1 of 9 patients with nonglioma CNS disease, and 2 of 34 *TERT* WT gliomas.

Within the limits of our cohort, we detected no significant correlation between *TERT* MAF in plasma and age, duration of symptoms, tumor grade, mutational status (*C228T*/*C250T*), tumor volume, contrast enhancement, overall survival and progression-free survival (Supplementary Fig. S4). However, we noted that patients with contrast enhancing tumors (increased breakdown of blood–brain barrier) tended to have higher MAF than patients with non-contrast–enhancing tumors (Supplementary Fig. S1G). Furthermore, patients with MAF above threshold tended to have poorer progression-free survival and overall survival compared to patients with below threshold MAF (Supplementary Fig. S1A and S1B).

We also report perfect concordance in 4 available matched CSF samples from both cohorts compared to a tissue gold standard (*TERT* mutant $n = 3$; *TERT* WT $n = 1$). We also detect a *TERT* mutation in the CSF of a patient sample whose plasma *TERT* MAF was below the defined assay threshold (Supplementary Fig. S5).

Detection of *TERT* promoter mutations in cfDNA for longitudinal monitoring

To assess the performance of the *TERT* assay in a longitudinal setting, we analyzed cfDNA from serial plasma samples of five patients with *TERT*-mutant glioma maintaining the same analytical parameters. *TERT*-mutant copies over the course of therapy paralleled imaging findings and clinical performance of patients (**Fig. 4**). Each of the patients had *TERT* mutant MAF above threshold prior to initial surgical resection and levels returned to baseline postoperatively. Patients P1 and P2 had stable disease with the *TERT*-mutant levels remaining below baseline over time. On follow up, 3 patients (P3, P4, P5) developed contrast enhancing lesions on MR images after chemoradiation. P4 and P5 had histopathologic confirmation of progression while P3 had clinically diagnosed progression. *TERT* MAF increased with the development of contrast-enhancing recurrent lesions coincident with clinical deterioration. Plasma from P4 was not available for analysis at the time of suspected disease progression.

Discussion

This study demonstrates for the first time, in a majority of glioma patients with a known tissue *TERT* promoter mutation, the detection of the same mutation in glioma patients' plasma, using a novel enhanced ddPCR assay. We report an overall sensitivity of 62.5% and a specificity of 90% of detecting cfDNA *TERT* promoter mutations in plasma compared with a matched tumor tissue gold standard in 114 patients with glioma. The ability to detect the highly prevalent *TERT* promoter mutation in the plasma of patients with glioma enhances our ability to diagnose, monitor and assess responses to therapy.

In this report, we overcome several challenges that have prevented detection of cfDNA point mutations in specific genes in the plasma of patients with brain tumor, including for the *TERT* promoter specifically. In contrast to other tumor types, where cfDNA point mutations are abundant, this is not the case in glioma. Several prior reports have detected specific oncogenic point mutations in cfDNA, including at the *TERT* promoter locus, in less than 5% of patients (5, 8, 26). This may be related to generally lower levels of CNS-derived circulating tumor DNA (ctDNA) in the blood, thought to be a function of the blood–brain barrier (BBB; ref. 5). While in our patient cohort, we show that tumor size does not correlate with plasma *TERT* MAF (similar to a prior report of non-specific cfDNA quantitation in glioma; ref. 27), we did note a tendency for patients with contrast-enhancing lesions

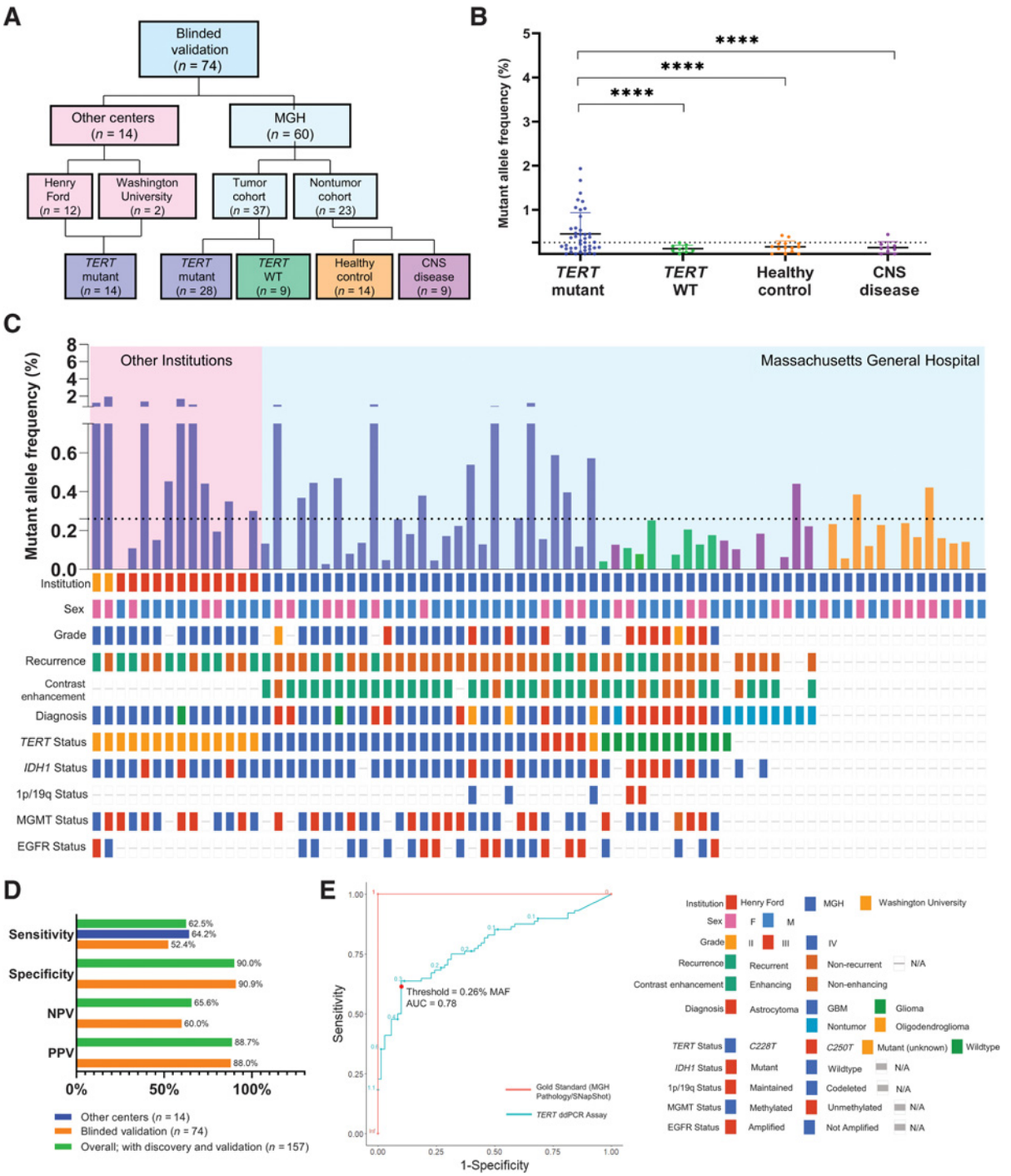

Figure 3.

Detection of *TERT* promoter mutation in plasma of blinded multi-institution validation cohort. **A,** CONSORT diagram depicting patient cohort and design of multi-institution validation cohort. **B,** cfDNA from 2 mL of matched patient plasma from blinded multi-institution cohort ($n = 74$; $n = 14$ outside institution, *TERT* Mutant, $n = 28$ MGH *TERT* Mutant, $n = 9$ MGH *TERT* WT, $n = 14$ MGH healthy control, $n = 9$ MRI-positive nontumor) was used as input for absolute quantification of *TERT* mutant and analyzed using the parameters established in the discovery cohort. Data are shown in MAF, calculated using the formula described in Methods and Supplementary Fig. 2. MAF for all samples is plotted against sub-classification of patient samples. ****, $P < 0.0001$. **C,** MAF for all *TERT*-mutant plasma samples are graphed according to sample number, with an accompanying Oncoprint that depicts sample source and genomic landscape. Dotted line indicates threshold of 0.26% MAF used to designate samples as *TERT* mutant positive or negative. **D,** Analytic parameters were calculated from contingency tables and reported. **E,** ROC curve depicting change in sensitivity and specificity according to varying threshold. Red point indicates threshold used for analysis, 0.26% MAF. Gold Standard (MGH Pathology/SNapShot) is plotted in red, and *TERT* ddPCR Assay is plotted in blue.

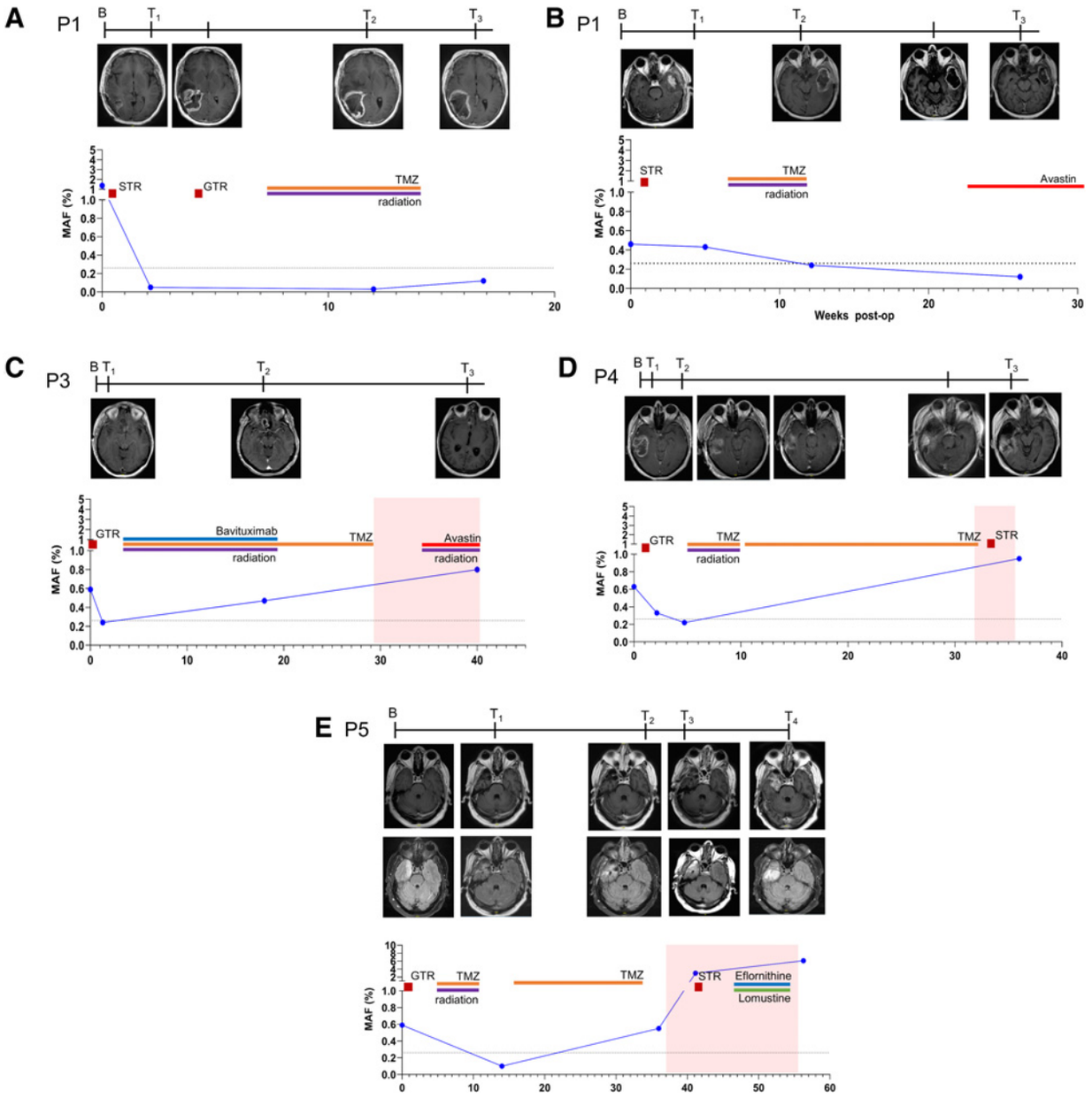

Figure 4.

Longitudinal monitoring of *TERT* promoter mutation in patients with glioma. *TERT* promoter mutation (copies/mL and MAF) in serial plasma samples obtained from 5 glioma patients is plotted against time (weeks post-op). Cases with stable disease include P1 (MGH-19038; grade IV *IDH1* wild-type GBM; **A**) and P2 (MGH-19006; grade IV *IDH1* wild-type GBM; **B**), and those with progression include P3 (MGH-18040; grade IV *IDH1* wild-type GBM; **C**), P4 (MGH-17045, grade IV *IDH1* mutant GBM; **D**), and P5 (MGH-18061; grade III, anaplastic astrocytoma; **E**). T1-weighted, contrast-enhanced MRI images are provided for timepoints when available. For P2, axial flair images are also provided. Timepoints are indicated as baseline (B), timepoint 1 (T1), timepoint 2 (T2), timepoint 3 (T3), and timepoint 4 (T4). Surgical procedures are indicated using a red square (STR, subtotal resection; GTR, gross total resection), orange line indicates administration of chemoradiation, and progression is indicated using a red background. Temozolomide, TMZ.

(indicative of BBB breakdown) to have higher plasma *TERT* MAF. Taken with the fact that recurrence timepoints (after surgery and chemoradiation) have more edema and higher plasma *TERT* MAF compared with baseline despite smaller tumor volumes, we hypothesize that plasma *TERT* MAF is correlated with breakdown of the BBB.

Our approach included several technical optimization strategies to detect low concentrations of *TERT* promoter mutations in plasma. Both *C228T* and *C250T* generate identical sequences, which can be detected with a single probe with LNA enhancements that stabilize probe-template duplexes to improve SNV discrimination. Furthermore, the *TERT* promoter region has a high GC-content (>80%) which we address by using 7-deaza-dGTP as a ddPCR additive, which interrupts the formation of these secondary structures. In combination, with standardized handling strategies and an unbiased analytic

method, we observed a significant improvement in assay sensitivity over previously published reports for *TERT* promoter detection in plasma of patients with glioma (28).

The challenge in detecting plasma cfDNA from patients with brain tumor highlights a missed opportunity for the advantages of the liquid biopsy approach in a tumor type where initial or repeat direct tissue sampling may pose substantial neurologic risk. While tissue biopsy will likely remain the gold standard for molecular diagnosis of glioma, the ability to detect oncogenic point mutations in the blood may have specific near-term application in two scenarios: (i) the described *TERT* promoter mutation assay may be useful for upfront diagnosis. Because some malignant tumors are located in deep or inaccessible locations and would be poor surgical candidates for direct tissue biopsy or resection, the combination of a characteristic set of MRI imaging findings in addition to a liquid biopsy that shows *TERT* promoter mutation may be sufficient to establish a high positive predictive value for the clinical diagnosis malignant glioma and allow adjunctive treatment with radiation and chemotherapy to proceed with confidence. (ii) In another scenario, because of the surgical risk of repeated brain biopsies, a liquid biopsy approach to *TERT* promoter mutation detection in the blood may be particularly suitable for therapeutic monitoring of disease burden, as exemplified conceptually in the longitudinal cases shown in this report. In our preliminary analysis, levels of *TERT* promoter mutants, as detected by this assay, do correlate with disease recurrence or progression. This can aid in differentiation between radiation necrosis, pseudoprogression, and true progression, thus minimizing the need for further invasive workup and improving overall quality of care. Furthermore, with emerging insights into intratumoral heterogeneity, the validity of a single, localized tissue biopsy as a true gold standard has begun to be debated (25), raising the possibility that a liquid biopsy, which effectively samples multiple tumor regions as blood perfuses the solid tumor mass, may offer greater sensitivity for *TERT* promoter mutation than a single, focal, tissue biopsy, in some patients.

Future studies offer the opportunity for further extension of this particular assay and the general approach of liquid biopsy for brain tumors. The false positive rate of our assay at the chosen MAF threshold was 10%, which is similar to the false positive rate of multimodality imaging analysis to infer diagnosis of gliomas. However, this also included assessment of patients with a very low predicted risk of glioma (e.g., healthy controls with no known MRI abnormalities and patients with fungal abscess/normal pressure hydrocephalus). In practical use, the *TERT* promoter mutation assay would be preferentially used in situations where disease prevalence is estimated to be high, for example, in patients with abnormal MRI scans consistent with glioma, To confirm the presence of glioma with a high positive predictive value. Within our cohort, 0 of 7 patients with an abnormal MRI and nonglioma CNS disease had *TERT* MAF above threshold. However, every patient with abnormal MRI (FLAIR and/or contrast abnormality) and a plasma *TERT* MAF above the threshold had a confirmed glioma diagnosis ($n = 55$ tissue *TERT* Mutant; $n = 2$ tissue *TERT* WT). This is especially true for patients with contrast-enhancing lesions on MRI and plasma *TERT* MAF above the threshold, as every patient in this subset also had a confirmed glioma diagnosis ($n = 42$ tissue *TERT* mutant; $n = 2$ tissue *TERT* WT). Thus, while our assay's sensitivity compared with a tissue gold standard is encouraging, future studies should assess the positive predictive value of the assay for the overall diagnosis of glial malignancy in the context of abnormal MRI findings. Furthermore, the combination of this plasma assay with advances in MRI imaging techniques that permit differentiation of various *TERT* promoter mutant glial tumors with different prognoses (e.g., glioblastoma vs. anaplastic oligodendroglioma) is also anticipated to be useful for clinical prognostication.

While our MAF threshold (0.26%) is optimized based on ROC analysis, from a clinical perspective, it is important to minimize the false positive rate of our assay (10%) below that of multimodal imaging. To this end, clinical studies across larger patient cohorts will be required to validate and standardize the gating parameters, plasma volumes, and clinical performance of the assay in heterogeneous populations with more extensive longitudinal sampling. These expanded studies should provide further insight on factors which produce false-negative and false positive results. Such factors may include assay MAF threshold performance in low prevalence populations (with potential false positives) or sampling of tumors with heterogeneous amounts of BBB breakdown (affecting cfDNA release), that manifest as false negative results in non-contrast–enhancing $TERT^{+}$ gliomas. Expanded studies will also allow further study of samples from multiple institutions; in the current report, the samples were heavily weighted (92%) from a single institution, potentially introducing bias in preanalysis sample handling with concomitant effects on assay performance.

The demonstration herein that the plasma detection of *TERT* promoter mutations in a majority of patients with glioma who harbor these tumor mutations opens the door to extending this to a multi-gene approach to further classify gliomas using a liquid biopsy approach, mimicking tissue-based molecular classification. This could be accomplished by careful optimization of assays for common glioma point mutations in the blood such as *IDH1* R132H mutations, EGFRvIII mutations, HK23M mutations and others. We also anticipate that this assay will also offer a sensitive method for detecting mutations in plasma cfDNA in other *TERT*-positive tumors.

In conclusion, we demonstrate a novel and highly sensitive ddPCR based *TERT* promoter mutation assay, utilizing high affinity LNA enhanced probes and the additive 7dG to reduce the formation of secondary structures, for detection and monitoring of *TERT* promoter mutations (*C228T*, *C250T*) in tumor tissue and cfDNA of matched plasma of patients with glioma with an overall sensitivity of 62.5% and a specificity of 90% in combined discovery and blinded validation cohorts of 157 samples. The ability to detect *TERT* mutations, which are highly prevalent in glioma patients, in the plasma enhances our ability to diagnose, monitor and assess response to therapy. Liquid biopsy-based monitoring can significantly impact clinical care by guiding patient stratification for clinical trials, offering new opportunities for the development of targeted therapies ultimately improving patient care.

Authors' Disclosures

K. Muralidharan reports a patent for *TERT* Promoter Droplet Digital PCR Assay For the Diagnosis of Malignant Cancer pending. A. Yekula reports a patent for *TERT* Promoter Droplet Digital PCR Assay for the Diagnosis of Malignant Cancers pending. S. Lau reports grants from United States Government during the conduct of the study. H. Lee reports grants from NCI and grants from DOD during the conduct of the study. C. Bettegowda reports personal fees from Depuy-Synthes and personal fees from Bionaut Labs outside the submitted work. M.R. Chicoine reports grants from IMRIS, Inc., The Head for the Cure Foundation, and Mrs. Carol Rossfeld and The Alex & Alice Aboussie Family Charitable Foundation during the conduct of the study. D.P. Cahill reports personal fees from Merck, Lilly, and Boston Pharmaceuticals outside the submitted work; in addition, D.P. Cahill has a patent 20170369939 pending and a patent 20190160139 pending. L. Balaj reports a patent for *TERT* Promoter droplet digital PCR Assay for the Diagnosis of Malignant Cancers pending. B.S. Carter reports a patent pending related to plasma-based detection of *TERT* mutations as described in this report. No disclosures were reported by the other authors.

Authors' Contributions

K. Muralidharan: Data curation, software, formal analysis, validation, investigation, visualization, methodology, writing-original draft, writing-review and editing. **A. Yekula:** Data curation, formal analysis, validation, investigation, visualization, methodology, writing-review and editing. **J.L. Small:** Investigation, writing-review and editing. **Z.S. Rosh:** Investigation, writing-review and editing. **K.M. Kang:** Investigation, writing-review and editing. **L. Wang:** Investigation, writing-review and editing. **S. Lau:** Investigation. **H. Zheng:** Formal analysis. **H. Lee:** Formal analysis, visualization. **C. Bettegowda:** Formal analysis, validation. **M.R. Chicoine:** Formal analysis, validation. **S.N. Kalkanis:** Formal analysis, validation. **G.M. Shankar:** Formal analysis, writing-review and editing. **B.V. Nahed:** Formal analysis, writing-review and editing. **W.T. Curry:** Writing-review and editing. **P.S. Jones:** Formal analysis, writing-review and editing. **D.P. Cahill:** Writing-review and editing. **L. Balaj:** Conceptualization, resources, data curation, software, formal analysis, supervision, funding acquisition, validation, investigation, visualization, methodology, writing-original draft, project administration, writing-review and editing. **B.S. Carter:** Conceptualization, resources, data curation, software, formal analysis, supervision, funding acquisition, validation, investigation, visualization, methodology, writing-original draft, project administration, writing-review and editing.

Acknowledgments

This work is supported by grants U01 CA230697 (to B.S. Carter, L. Balaj), UH3 TR000931 (to B.S. Carter), P01 CA069246 (to B.S. Carter), and R01 CA239078, CA237500 (to B.S. Carter, L. Balaj, H. Lee). The funding sources had no role in the writing of the manuscript or decision to submit the manuscript for publication. The authors have not been paid to write this article by any entity. The corresponding author has full access and assumes final responsibility for the decision to submit for publication. The authors thank all of the MGH Neurosurgery clinicians and staff who assisted with the collection of samples. They also thank the patients and their families for their participation in this study. They thank Alexandra Beecroft and Abigail Taylor for editorial help. They also thank Alona Muzikansky for help with the statistical analysis and Gur Rotkop and Sharmistha Chakrabortty for help with computational analysis.

The costs of publication of this article were defrayed in part by the payment of page charges. This article must therefore be hereby marked *advertisement* in accordance with 18 U.S.C. Section 1734 solely to indicate this fact.

Received August 5, 2020; revised September 15, 2020; accepted October 8, 2020; published first October 13, 2020.

References

1. Louis DN, Perry A, Reifenberger G, von Deimling A, Figarella-Branger D, Cavenee WK, et al. The 2016 world health organization classification of tumors of the central nervous system: a summary. Acta Neuropathol 2016;131:803–20.
2. Wang Y, Springer S, Zhang M, McMahon KW, Kinde I, Dobbyn L, et al. Detection of tumor-derived DNA in cerebrospinal fluid of patients with primary tumors of the brain and spinal cord. Proc Natl Acad Sci U S A 2015;112:9704–9.
3. Chen WW, Balaj L, Liau LM, Samuels ML, Kotsopoulos SK, Maguire CA, et al. BEAMing and droplet digital PCR analysis of mutant IDH1 mRNA in glioma patient serum and cerebrospinal fluid extracellular vesicles. Mol Ther Nucleic Acids 2013;2:e109.
4. Miller AM, Shah RH, Pentsova EI, Pourmaleki M, Briggs S, Distefano N, et al. Tracking tumour evolution in glioma through liquid biopsies of cerebrospinal fluid. Nature 2019;565:654–8.
5. Bettegowda C, Sausen M, Leary RJ, Kinde I, Wang Y, Agrawal N, et al. Detection of circulating tumor DNA in early- and late-stage human malignancies. Sci Transl Med 2014;6:224ra24.
6. Shankar GM, Francis JM, Rinne ML, Ramkissoon SH, Huang FW, Venteicher AS, et al. Rapid intraoperative molecular characterization of glioma. JAMA Oncol 2015;1:662–7.
7. Zill OA, Banks KC, Fairclough SR, Mortimer SA, Vowles JV, Mokhtari R, et al. The landscape of actionable genomic alterations in cell-free circulating tumor DNA from 21,807 advanced cancer patients. Clin Cancer Res 2018;24:3528–38.
8. Piccioni DE, Achrol AS, Kiedrowski LA, Banks KC, Boucher N, Barkhoudarian G, et al. Analysis of cell-free circulating tumor DNA in 419 patients with glioblastoma and other primary brain tumors. CNS Oncol 2019;8:CNS34.
9. Eckel-Passow JE, Lachance DH, Molinaro AM, Walsh KM, Decker PA, Sicotte H, et al. Glioma groups based on 1p/19q, IDH, and TERT promoter mutations in tumors. N Engl J Med 2015;372:2499–508.
10. Labussière M, Di Stefano AL, Gleize V, Boisselier B, Giry M, Mangesius S, et al. TERT promoter mutations in gliomas, genetic associations and clinico-pathological correlations. Br J Cancer 2014;111:2024–32.
11. Colebatch AJ, Witkowski T, Waring PM, McArthur GA, Wong SQ, Dobrovic A. Optimizing amplification of the GC-Rich TERT promoter region using 7-Deaza-dGTP for droplet digital PCR quantification of TERT promoter mutations. Clin Chem 2018;64:745–7.
12. Bell RJA, Rube HT, Xavier-Magalhaes A, Costa BM, Mancini A, Song JS, et al. Understanding TERT promoter mutations: a common path to immortality. Mol. Cancer Res 2016;14:315–23.
13. Colebatch AJ, Dobrovic A, Cooper WA. TERT gene: its function and dysregulation in cancer. J. Clin. Pathol 2019;72:281–4.
14. Killela PJ, Reitman ZJ, Jiao Y, Bettegowda C, Agrawal N, Diaz LA, et al. TERT promoter mutations occur frequently in gliomas and a subset of tumors derived from cells with low rates of self-renewal. Proc Natl Acad Sci U\ S A 2013;110:6021–6.
15. Vinagre J, Almeida A, Pópulo H, Batista R, Lyra J, Pinto V, et al. Frequency of TERT promoter mutations in human cancers. Nat. Commun 2013;4:2185.
16. Kang S, Ohshima K, Shimizu M, Amirhaeri S, Wells RD. Pausing of DNA synthesis in vitro at specific loci in CTG and CGG triplet repeats from human hereditary disease genes. J Biol Chem 1995;270:27014–21.
17. Motz M, Pääbo S, Kilger C. Improved cycle sequencing of GC-rich templates by a combination of nucleotide analogs. BioTechniques 2000;29:268–70.
18. Mamedov TG, Pienaar E, Whitney SE, TerMaat JR, Carvill G, Goliath R, et al. A fundamental study of the PCR amplification of GC-rich DNA templates. Comput Biol Chem 2008;32:452–7.
19. McEvoy AC, Calapre L, Pereira MR, Giardina T, Robinson C, Khattak MA, et al. Sensitive droplet digital PCR method for detection of TERT promoter mutations in cell free DNA from patients with metastatic melanoma. Oncotarget 2017;8:78890–900.
20. Corless BC, Chang GA, Cooper S, Syeda MM, Shao Y, Osman I, et al. Development of novel mutation-specific droplet digital PCR assays detecting TERT promoter mutations in tumor and plasma samples. J. Mol. Diagn 2019;21:274–85.
21. Attali D, Bidshahri R, Haynes C, Bryan J. ddpcr: an R package and web application for analysis of droplet digital PCR data. F1000Research 2016;5:1411.
22. Zheng Z, Liebers M, Zhelyazkova B, Cao Yi, Panditi D, Lynch KD, et al. Anchored multiplex PCR for targeted next-generation sequencing. Nat Med 2014;20:1479–84.
23. Juratli TA, Thiede C, Koerner MVA, Tummala SS, Daubner D, Shankar GM, et al. Intratumoral heterogeneity and promoter mutations in progressive/higher-grade meningiomas. Oncotarget 2017;8:109228–37.
24. Nakajima N, Nobusawa S, Nakata S, Nakada M, Yamazaki T, Matsumura N, et al. BRAF V600E, TERT promoter mutations and CDKN2A/B homozygous deletions are frequent in epithelioid glioblastomas: a histological and molecular analysis focusing on intratumoral heterogeneity. Brain Pathol 2018;28:663–73.
25. Sottoriva A, Spiteri I, Piccirillo SGM, Touloumis A, Collins VP, Marioni JC, et al. Intratumor heterogeneity in human glioblastoma reflects cancer evolutionary dynamics. Proc Natl Acad Sci U S A 2013;110:4009–14.
26. Juratli TA, Stasik S, Zolal A, Schuster C, Richter S, Daubner D, et al. TERT promoter mutation detection in cell-free tumor-derived DNA in patients with IDH wild-type glioblastomas: a pilot prospective study. Clin Cancer Res 2018;24:5282–91.
27. Nørøxe DS, Østrup O, Yde CW, Ahlborn LB, Nielsen FC, Michaelsen SR, et al. Cell-free DNA in newly diagnosed patients with glioblastoma - a clinical prospective feasibility study. Oncotarget 2019;10:4397–406.
28. Juratli TA, Stasik S, Zolal A, Schuster C, Richter S, Daubner D, et al. Promoter mutation detection in cell-free tumor-derived DNA in patients with wild-type glioblastomas: a pilot prospective study. Clin Cancer Res 2018;24:5282–91.